A HIGH ALTITUDE GROUND-BASED CLOUD SEEDING EXPERIMENT CONDUCTED IN SOUTHERN UTAH

Arlen W. Huggins
Desert Research Institute
Reno, Nevada 85906

and

Ken Sassen
University of Utah
Salt Lake City, Utah 84112

Abstract. A wintertime ground-based cloud seeding experiment conducted as part of the 1989 Utah/NOAA cooperative weather modification program is described. The results from one experiment on 3 February 1989 are presented. Meteorological conditions led to the development of orographic clouds over the Tushar Mtns of southern Utah which appeared to be nearly ideal for seeding operations. Radiometrically measured liquid water was abundant in the vicinity of seeding generators and the water appeared to be sufficiently supercooled to enable nucleation by silver iodide.

The experiment entailed pulsed releases of silver iodide from high altitude generators located on upwind ridges of the Tushar Mtns. A K_a-band radar, aspirated PMS 2D-C probe, and manual microphysics observations were used to monitor precipitation 10-13 km downwind of the seeding generators. Snow samples were also collected periodically and analyzed for silver content. The overall results were disconcerting in that two estimated periods of effect showed no enhanced silver content, and no clear microphysical or radar seeding signatures due to large background variability produced by a propagating mesoscale cloud feature, and natural snow characteristics which resembled the expected characteristics due to seeding. A third period of effect had apparent microphysical and radar signatures, but also lacked the presence of silver in the snow. Targeting of the single downwind ground target apparently failed in this case due to inadequate wind documentation in the cloud layer, remote-generator malfunction, or fallout of the seeded plume upwind of the target.

1. INTRODUCTION

As part of the Federal/State cooperative weather modification research program the Utah Division of Water Resources, in cooperation with the National Oceanic and Atmospheric Administration (NOAA), has conducted several field research programs on winter storms in the Tushar Mtns of southwestern Utah. The research has been designed to enhance the understanding of cloud formation and evolution over mountainous terrain, to study the transport and diffusion of ground released cloud seeding material and to improve the operational winter snowpack augmentation project conducted by Utah.

The existence of supercooled liquid water is a necessary condition for successful cloud seeding operations. As such, prior to 1989 the Utah/NOAA field studies concentrated on documenting the characteristics of supercooled liquid water in a wide variety of storms, primarily using remote sensing instrumentation such as a lidar and microwave radiometer. Long (1986) discusses some of these results and notes that nearly all storms contained periods where liquid water existed in clouds over the Tushar Mtns, with the liquid cloud bases being generally less than 200-300 m above the terrain and at temperatures colder than -5°C. Recently, seeding experiments in wintertime clouds over the Sierra Nevada (Deshler et al., 1990) have shown significant ice crystal production (>100 l^{-1}) using one silver iodide compound at -6C. The advantages for ground-based seeding with such warm temperature activation are obvious. Sassen et al. (1990) shows that the liquid water in clouds over the Tushars can be influenced by small-scale terrain features and provides a conceptual model of orographic storm conditions that are apparently favorable for cloud seeding operations.

Some limited studies of seeding material transport into clouds over the Tushars have also been conducted and, although these are not conclusive to date, preliminary indications are that material released from the ground has a better chance of being vertically transported to supercooled regions of clouds when the seeding generators are positioned at relatively high altitudes, as opposed to valleys where inversions and blocked flow conditions often inhibit material transport (Long, 1984, 1986). Super and Boe (1988) and Super and Heimbach (1988) have documented seeding effects from high altitude ground-based generators in mountainous regions of Colorado and Montana.

Seeking to take advantage of the knowledge gained concerning the location of liquid water in the Tushars, and the success in targeting clouds in other mountainous regions, the Utah/NOAA field program in 1989 concentrated on ground-based seeding experiments using generators located both on the upwind slopes of the Tushar Mtns themselves and on separate mountain ridges to the southwest and west of the Tushars. This paper describes the results of test seeding using the generators located in the Tushars, within 13 km of an instrumented target site. Measurements at the target were used to attempt to identify microphysical changes in

precipitation induced by seeding (seeding signatures).

2. SEEDING EXPERIMENT METHODOLOGY

2.1 Experimental Hypotheses

The hypotheses used by the Utah operational winter cloud seeding project are similar to the ones tested during the 1989 Utah/NOAA research program. The scientific hypotheses empirically tested in 1989 were:

Hypothesis 1: Silver iodide seeding material can be delivered to clouds of supercooled liquid water over the Tushar Mtns from ground generators operating high on the upwind slopes of these same mountains.

Hypothesis 2: The silver iodide seeding material, through ice nucleation and the precipitation processes of deposition, riming, and/or aggregation, will lead to additional numbers of precipitation particles within the clouds.

Hypothesis 3: The additional precipitation particles will fall along trajectories which carry them to an instrumented site in the Tushar Mtns.

2.2 Operational Approach

Figure 1 shows the disposition of equipment used in the experiment. Four remotely controlled generators were positioned at the sites indicated by the solid triangles (Fig.1 and Table 1). The generators used a 3% by weight solution of AgI-NH_4I in acetone burned in a propane flame. The positioning of these generators relative to the Upper Grizzly Ridge target site (UGR) was based on the previously documented association of liquid water occurrence with winds from the south through west (Rauber and Grant, 1988). The generator spacing was believed sufficient to target UGR, provided the angular horizontal plume dispersion was 15° or more. Such dispersion from ground sources has been documented by Holroyd et al. (1988) and Super and Heimbach (1988). Multiple generators were operated during experiments to account for wind variations and increase the likelihood of affecting the target. Seeding generators were also pulsed on and off at intervals of 1-1.5 h. This was done to significantly increase the number of seed and no-seed periods, and improve the chances of noting seeding effects in post-analysis.

The microwave radiometer was positioned at about midbarrier (Fig. 1) to measure the liquid water in clouds forming in the region near the seeding generators. Long (1986) and Sassen et al. (1990) show that several azimuth sectors within the western semicircle of the scanning radiometer frequently contain enhanced amounts of liquid water due to the lifting of moist air over sharply rising terrain in those directions. A K_a-band radar was positioned downwind of the generators at

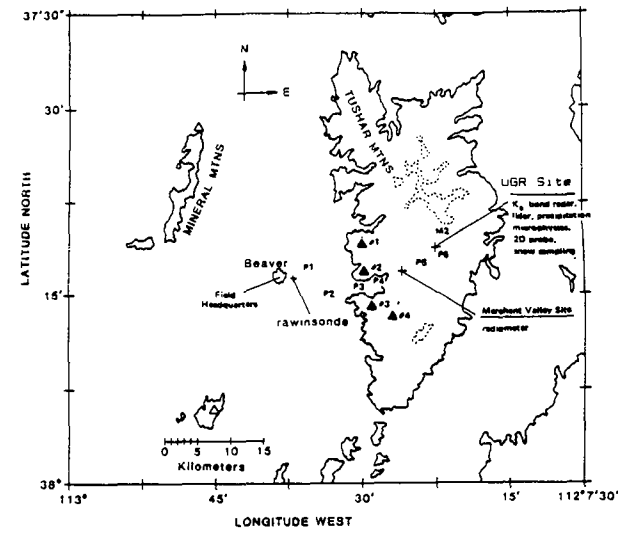

Figure 1. Locations of the instrumentation in the 1989 UT/NOAA Field Research Program. Symbols P1, P2, ...P7 indicate precipitation gage sites. Closed triangles numbered 1-4 are sites of remote-controlled silver iodide generators. Terrain contours are 2438 m MSL (solid line) and 3353 m MSL (dashed line).

UGR. This site was also equipped with an aspirated 2D-C optical array probe, a high resolution precipitation gage, and instrumentation for microphysical and chemical sampling of the precipitation.

Each experiment was conducted when certain cloud and meteorological criteria were met. These criteria are listed in Table 2. They reflect the belief that seeding effects would be greatest when: a) clouds have relatively warm tops and therefore possibly less natural ice, but are cold enough for silver iodide activation, b) precipitation is light and forms a low background against which to measure seeding effects, c) supercooled liquid water is present in relatively large amounts and therefore is sufficient to support substantial growth of particles to precipitation sizes, d) cloud bases are sufficiently low to cover the generator sites and ensure delivery of the seeding material directly into the clouds, and e) winds at the height of the upper part of the Tushar Mtns have a direction that will carry seeding effects toward UGR. The criteria were meant to ensure that clouds were suitable for seeding and also that the set of experiments would contain a relatively homogeneous sample of clouds.

2.3 Detection of Seeding Effects

The detection of seeding effects involved a test of each of the three experimental hypotheses. The experiment was designed to ensure that AgI was unambiguously delivered to clouds over the Tushars. Visual and radiometric observations were made to ensure that seeding criteria d was satisfied, thus partially confirming Hypothesis 1. Confirmation of material delivery was also dependent on

Table 1. Remote generator altitudes (MSL) and locations relative to the UGR target site at 2975 m altitude.

Remote Site	Altitude (km)	Direction from UGR (deg)	Distance from UGR (km)	Time from UGR at 10 m s^{-1}
1	2.88	266.5	10.3	17.2 min
2*	2.79	248.0	8.7	14.5 min
3	2.58	228.5	13.6	22.7 min
4	3.25	204.0	13.2	22.0 min

* Site 2 was inoperative during the entire 1989 Field Program

Table 2. Criteria for initiating Research Seeding Experiments

Variable	Limits	System
Time of Day	0000 - 2400 MST	
Wind Direction (2.5-3.5 km MSL)	195 - 276 deg	Rawinsonde
Wind Speed	5.0 - 12.5 m s^{-1}	Rawinsonde
Integrated LW	> 0.10 mm	Radiometer
LW Height	< 2.80 km	Visual Rawinsonde
LW Temperature	< -5 °C	Rawinsonde
Clouds	St, StCu, Cap Cloud	Visual Satellite
Precipitation	< 1.0 mm h^{-1}	Snow Mass Sampling
Cloud Top Temp.	> -20 °C	Satellite K_a-band Sounding

knowledge that the remote generators operated properly. Information obtained in real time by coded radio signals relayed to the operations center indicated whether or not a burner was operating and the AgI solution valve was open or closed. Although generator tests on days prior to and following experiments confirmed proper operation, there was still an uncertainty associated with proper operation during an experiment, in that solution flow could not be confirmed in real time. Given this one uncertainty in confirming Hypothesis 1, the times when generators were pulsed on and off were then used, along with an estimate of seeding material and precipitation particle transport times using rawinsonde winds, to estimate when seeding effects might be observed above the radiometer and at UGR. These periods of effect (POE) were then used to focus the tests of Hypotheses 2 and 3 on the appropriate segments of radiometer and UGR data sets.

Confirmation of Hypothesis 2 required the observation of additional precipitation particles within the cloudy volume downwind of the seeding generator sites. Since no in situ observations were available, the K_a-band radar, operated in zenith pointing mode at UGR, provided the primary means of confirming this hypothesis. A lidar, which was also intended to be used, was not operational during the experiments described here. This reliance on remote sensing instruments obviously limited the ability to confirm Hypothesis 2, especially between the generators and UGR. Recent successes in documenting physical seeding effects in-cloud have relied on aircraft data (e.g., Super and Boe, 1988), or a combination of aircraft and radar data (e.g., Deshler et al., 1990).

Reflectivity factors above the radar before, during, and after POE's were compared. Seeding effects might have appeared as increased reflectivity fac-

tors. In general, an increase in radar reflectivity ($Z = ND^6$) can result from a change in concentration (N), or size (D). For example, if seeding creates a large number of small particles, say 20 l^{-1} of 100 micron diameter (water sphere equivalent), the contribution to the ice-relative Z_i (see Sassen, 1987) is only 0.0236 $mm^6\ m^{-3}$ or -16 dBZ_i. However, if aggregates in concentration of 1 l^{-1} with 0.5 mm equivalent diameter are formed, the contribution is 18.45 $mm^6\ m^{-3}$ or about 13 dBZ_i. Since previous successes in detecting radar seeding signatures have occurred primarily in clouds with little or no natural echo (see Deshler et al., 1990), "seeding signatures" were only expected in clouds with negligible natural precipitation.

Seeding effects in radiometer data might appear as a depletion of the supercooled liquid water in clouds passing over the radiometer site. To date no such effects have been documented, but data from periods when seeded plumes were expected to be over the radiometer were compared with unseeded time periods.

Confirmation of Hypothesis 3 required that additional precipitation particles were observed at UGR during the POE. The precipitation microphysics, K_a-band radar data, and snow chemistry data were used to attempt this confirmation. All data were plotted as a function of time so data within the POE could be compared to unseeded periods. A given POE was expected to show some or all of the following characteristics:

a) an increased concentration of individual precipitation particles (ice crystals) predominantly in the small size categories (< 500 microns), due to the typically short growth time (<1000 s) available between a generator and UGR,
b) an increased concentration of aggregates of crystals, and possibly a greater mean aggregate size,
c) individual particle (crystal) sizes appropriate to the estimated growth time and growth rate,
d) individual particle habits appropriate to a depositional growth temperature and humidity approximately intermediate to that of the seeding site and UGR, and
e) increased precipitation rate (mass flux).

Measurements were made of the silver content of the snow at UGR during all experiments, at approximately 15-min intervals. During the design of the field experiment, four possible combinations of silver concentration and microphysical observations were hypothesized for a POE. First, silver above background might be detected with none of the expected microphysical effects. This would suggest that silver probably arrived through scavenging, and seeding did not cause microphysical effects at UGR. Second, no silver is detected and no microphysical effects are observed. This would suggest that either directional targeting of UGR failed, or seeding effects were produced entirely upwind of, or downwind of UGR. Third, no silver is detected but some evidence of microphysical effects exist. This would suggest that targeting failed, but effects produced by natural cloud processes occurred by chance during the POE. Fourth, silver above background and microphysical effects might be detected in a temporally consistent manner. This would be strong evidence that seeding effects occurred at UGR. These hypothetical results will be compared to actual observations.

3. SEEDING EXPERIMENT FOR 3 FEBRUARY 1989

Pulsed seeding experiments using the high altitude generators were conducted on five separate occasions during the 1989 Utah/NOAA field program (1 February - 15 March). Each Research Seeding Experiment (RSE) began when the criteria in Table 2 were observed to be met. Data were always collected for one hour at the beginning of an RSE before any actual seeding began. This allowed for a period of natural background data, particularly Ag concentrations, for comparison with the first POE. Then, based on wind information from rawinsondes taken at Beaver (Fig. 1), one or more generators were selected for use and alternatingly turned on and off for periods of 0.5 - 1.5 h, lasting altogether about five hours. Rawinsonde winds could obviously not account for the complexity of flow over the mountainous terrain, but prior studies in the Tushar Mtns using a Doppler radar at midbarrier (Snider et al., 1986) showed reasonable agreement in wind direction and speed above 3 km MSL between Doppler winds and rawinsonde winds. Below 3 km Doppler winds were generally slower than rawinsonde winds, and directions were more variable. The RSE ended with another no-seed period, so the total intended length of each RSE was seven hours. Some experiments were terminated sooner when seeding criteria were no longer observed to be met.

The seeding experiment (RSE#1) conducted on 3 February was selected for initial analysis based on indications of seeding effects at UGR in real time. The following discussion documents that case study in detail.

3.1 Meteorological Conditions

RSE#1 was conducted from 0900 (all times MST) to 1615 on 3 February, during a longer stormy period which started at 2100 on 2 February and ended at 2100 on 4 February 1989. The main synoptic features of the storm were an upper level closed low which was located slightly west of the Oregon coast, and an arctic cold front which was situated across northern Utah at the beginning of the storm. To the southeast of the closed low, southern Utah was under the influence of southwesterly winds at 500 and 700 mb, and was affected by one

or more minor shortwaves which rotated around the slowly moving low center.

For the period which included RSE#1, moisture was advected into southern Utah from the southwest, and weak cold air advection occurred with the passage of one of the shortwaves. The upper air station at Desert Rock in southern Nevada showed a decrease in temperature at 700 mb from -2C to -6C between 0500 on 2 February and 1700 on 3 February. During the same period a region of low dewpoint depression moved into western Utah such that by 0500 on 3 February the Utah/NOAA project area was near the boundary of air whose dew point depression was less than 3°. Figure 2 shows the 700 mb height/temperature pattern for 1700 on 3 February. A shortwave trough axis was near the Utah/Nevada border with the stronger cold advection over southern California and Nevada.

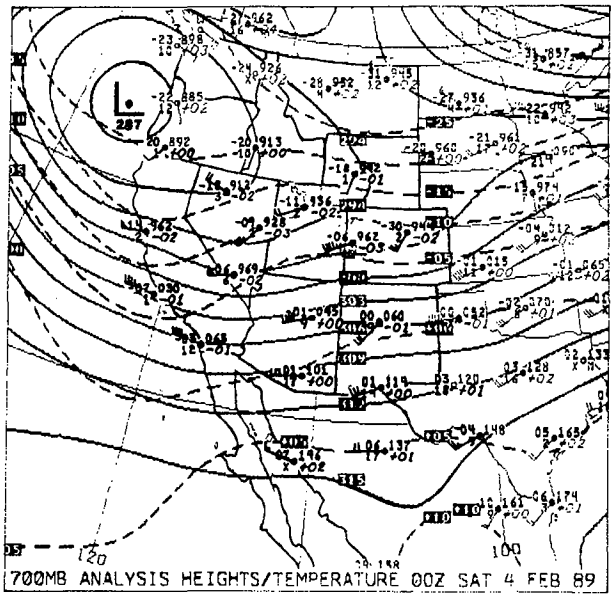

Figure 2. 700 mb analysis of geopotential height, temperature, and wind for 1700 MST on 3 February 1989.

In southern Utah the storm began with the development of a nearly nonprecipitating midlevel cloud deck during the night of 2 February. Throughout the day of 3 February an orographic cloud persisted over the Tushar Mtns. Satellite images and visual observations from Beaver revealed considerable mesoscale structure in the clouds during the morning and afternoon of 3 February. Visible satellite images (not shown) from 1200 to 1230, near the midpoint of the RSE#1 period, showed low-level clouds which appeared to have been enhanced over many of the mountain barriers in southern Utah.

3.2 Local Atmospheric Structure and Seeding Criteria Verification

Four soundings were taken from Beaver during the storm, but only three provided good low-level wind information. Figure 3 shows the contoured fields of tempera-

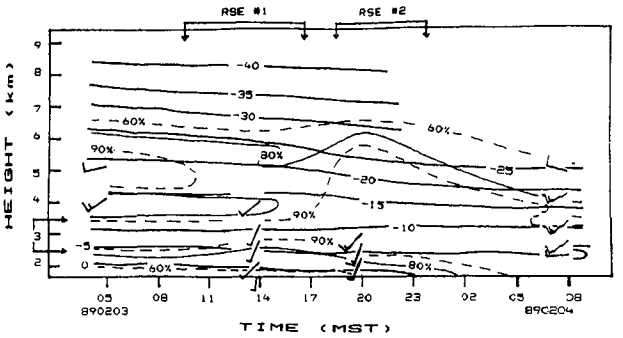

Figure 3. Time versus height plot of temperature and relative humidity for 3-4 February 1989, based on soundings at 0500, 1400, and 2000 on 3 Feb, and 0800 on 4 Feb. Wind barbs are 10 m/s and 5 m/s. Height region where seeding criteria were evaluated is shown by arrows on height scale.

ture and relative humidity, and wind barbs in time versus height format for the storm period encompassing RSE#1 and RSE#2 (noted above top panel). RSE#2 is not considered here due to the lack of some of the supporting data at UGR. The brackets on the vertical scale denote the region where seeding criteria were evaluated. For RSE#1 the bottom of this layer was -5 to -6°C with the top at -11 to -12°C. This layer was also at or greater than 90% relative humidity. The sounding at 1400 indicated a lifting condensation level around 2.8 km MSL, quite near the level required for the base of liquid water in Table 2. With liquid base at this level, the temperature criteria of Table 2 would also be satisfied. Based on the 1400 sounding, wind speed in the 2.5-3.5 km layer met the criteria, averaging 5.2 m s^{-1}. Wind direction was close to the southerly limit of 195°, ranging from 200-204° with an average of 202°. Note that these winds are significantly more southerly than the 700 mb winds shown over southern Utah in Fig. 2 at 1700. Previous studies (Huggins, 1989) have shown that winds from the southwest, at levels below the Tushar crest, back as much as 20° in response to the presence of the mountain barrier.

Between 0830 and 0900 on 3 February cloud base was confirmed to be below the height of the seeding generators by visual observations from the radiometer location. Radiometer liquid depth exceeded 0.10 mm, the cloud over the Tushars resembled an extended barrier cap cloud (Sassen et al., 1990), and the precipitation rate at UGR was well below 1 mm h^{-1}. RSE#1 was therefore initiated at 0900 based on these real-time observations. Table 3 shows the seeding times and the conditions at seeding Generator 4 during RSE#1. Only Generator 4 on a 204° azimuth from UGR is presented because the south-southwesterly winds indicate it would likely have been the only generator to target UGR. The cloud conditions, and the real-time information that the seeding generators operated properly (provided the solution line was not clogged), indicated that Hypo-

Table 3. On and off time periods for Generator 4 during RSE#1 with temperature and liquid water averages during the on times.

Time Period (MST on 2/3)	Generator 4 Mode	Radiometer Avg. LW Depth (mm)	Radiometer LW Conc. for 1-km depth (g m^{-3})	Temperature at Gen.4 (°C)
0900 - 1000	OFF	---	---	---
1002 - 1130	ON	0.30	0.30	-9.5
1130 - 1230	OFF	---	---	---
1230 - 1330	ON	0.70	0.70	-9.5
1330 - 1430	OFF	---	---	---
1430 - 1530	ON	0.25	0.25	-9.5
1530 - 1615	OFF	---	---	---

thesis 1 was satisfied.

3.3 Estimation of the Seeding Period of Effect (POE)

Advection time between Generator 4 and UGR provides a means of determining the estimated POE's. This involves the assumption that the rawinsonde winds measured from the upwind location were also appropriate for regions over the barrier. Since no other wind measurements existed, and since the sounding showed little speed or directional shear in the cloud layer (limited to region below 3.5 km), this method of determining the POE is probably as good as is possible from the available data. Using the mean wind of 202° at 5.2 m s^{-1}, the travel time from Generator 4 to UGR is 42.3 min. This provides the following POE's:

POE1 = 1044-1212 MST
POE2 = 1312-1412 MST
POE3 = 1512-1612 MST.

A 1 m s^{-1} uncertainty in wind speed alters the start/end times by plus or minus 7 min.

Based on observations of seeding effects at similar seeding temperatures during the Sierra Cooperative Pilot Project (Deshler et al., 1990) and recent model results of Prasad et al. (1989), a reasonable seeding effect after about 40 min would be the appearance of rimed, nearly spherical particles, in the 600 to 700 micron size range. Both observations and model results indicate riming to be the dominant growth mechanism for crystals nucleated at -10C, about 5 min after nucleation, for liquid water contents as low as 0.05 g m^{-3}. Fukuta (1980) also points to this temperature as favorable for graupel formation due to the equidimensional crystal that is produced. For this situation aggregation may not be an important factor.

3.4 Search for Seeding Effects at UGR

Figure 4 presents the radar and 2D-C data from the UGR site for a period encompassing RSE#1. Radar reflectivity is displayed in dBZ$_i$ (assumes Rayleigh scattering of ice particles with $[K]^2i = 0.176$) in 5 dB intervals beginning at -10 dBZ$_i$. Seeding generator on-times are noted by the brackets below the radar data. The total 2D-C concentration, after artifact and zero-area image rejection, is shown in the second panel of Fig.4, along with an estimated 2D-C precipitation rate based on a mass-diameter relationship used by Holroyd (1987). The precipitation rate curve should only be considered in a relative sense since the mass relationships have not been adjusted (as suggested by Holroyd, 1987) for the type of snowfall in our geographic region. The third panel shows the contribution to concentration by size category, and the fourth panel shows the contribution by particle habit. The habit categories were also identified using the technique of Holroyd (1987). Manual microphysics observations from UGR and radiometer liquid water depth from Merchant Valley are shown in Fig. 5. The second panel displays precipitation rates determined from snow mass samples collected for chemical analysis at about 15 minute intervals. The collecting device had a diameter of 127 cm. Samples were analyzed for silver content using the technique of Warburton et al. (1982). Each sample was divided into parts and analyzed 3-5 times. The average and sample standard deviation of silver concentration for each sample is plotted in the second panel of Fig. 5. The bottom panel of Fig. 5 contains particle number flux estimates determined from counting particles over known areas of black velvet which had been exposed to snowfall for known periods of time.

3.4.1 Period of Effect 1

Prior to and during the first half of POE1 two radar echo layers were present; 4.6 km (-17C) to 6.0 km (-25C), and from the surface to 4.2 km (-13C). The low level echo which was present before seeding began showed no significant change in structure through the beginning of POE1. The two layers merged at 1145 as a prominent echo band arrived and the base of the upper layer descended from 4.5 km to the surface between 1100 and 1150, near the end of POE1. The 2D-C concentration was relatively steady at 7-20 l^{-1} before and through the first half of POE1, with no increase in concentration which would have indicated a seeding effect. Less than 10% of the particles were >400 microns in diameter. One noticeable peak in the 200-400 micron sizes occurred at 1100 during POE1, but declining numbers of large sizes led to a decline in 2D-C precipitation through 1130.

Particle habits (not shown) indicated that the precipitation prior to 1130 came mainly from the warmer cloud layer. Particles were mostly very small (<500 microns), nearly spherical, rimed particles. These habits matched what was expected as a result of seeding. An occasional broken dendritic branch suggested there were brief episodes of interaction with the colder cloud layer. After 0915 the precipitation rate was less than 0.1 mm h^{-1}. (Note the 2D-C computed precipitation in Fig. 4 underestimates by a factor of 4-7 throughout RSE#1.) A minor precipitation rate peak is shown in Fig. 5 at the beginning of POE1. Particle number flux (Fig. 5, bottom panel) had a corresponding minor peak as did small particles and hexagonal habits in the 2D-C plot in Fig. 4. How-

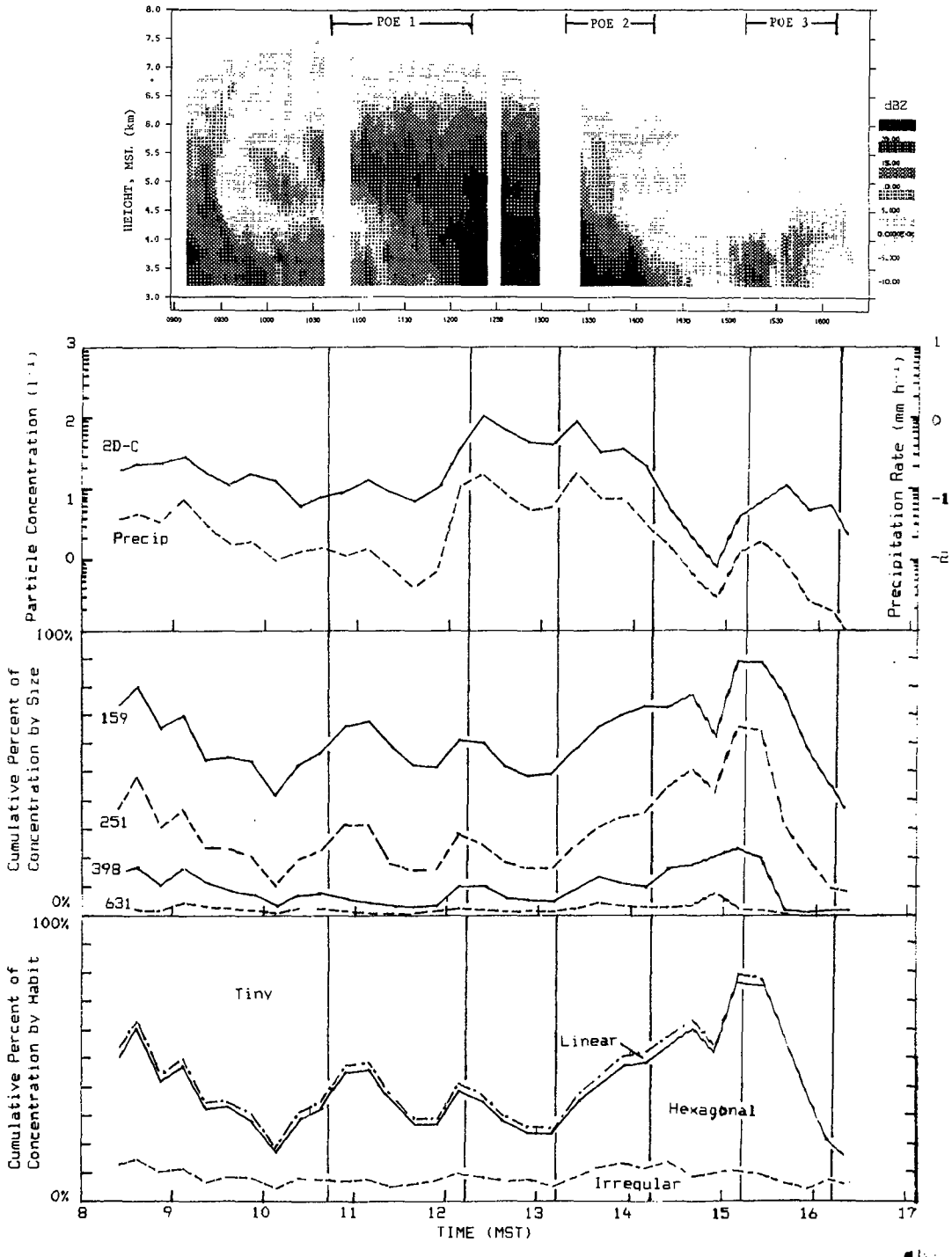

Figure 4. Time series plots of Ka-band radar data (top panel), 2D-C concentration and estimated precipitation (second panel), cumulative percent of 2D-C concentration by size in micrometers (third panel), and cumulative percent of 2D-C concentration by habit category (bottom panel). Estimated seeding periods of effect (POE) are indicated at the top of the radar panel.

ever, the increase in small and hexagonal particles began at about the time seeding began.

The arrival of the radar echo band is quite obvious just at the end of POE1. Particle number flux increased an order of magnitude, as did 2D-C concentration and precipitation rate. The liquid water depth, which had been 0.2 to 0.45 mm prior to the echo band, began rising sharply at 1130, about 30 min before the increase in precipitation at UGR.

Although there was some similarity to the expected seeding effects in the observed particle habits and sizes, the timing was not consistent with the start of the POE, and total concentration increases were only minor. The lack of

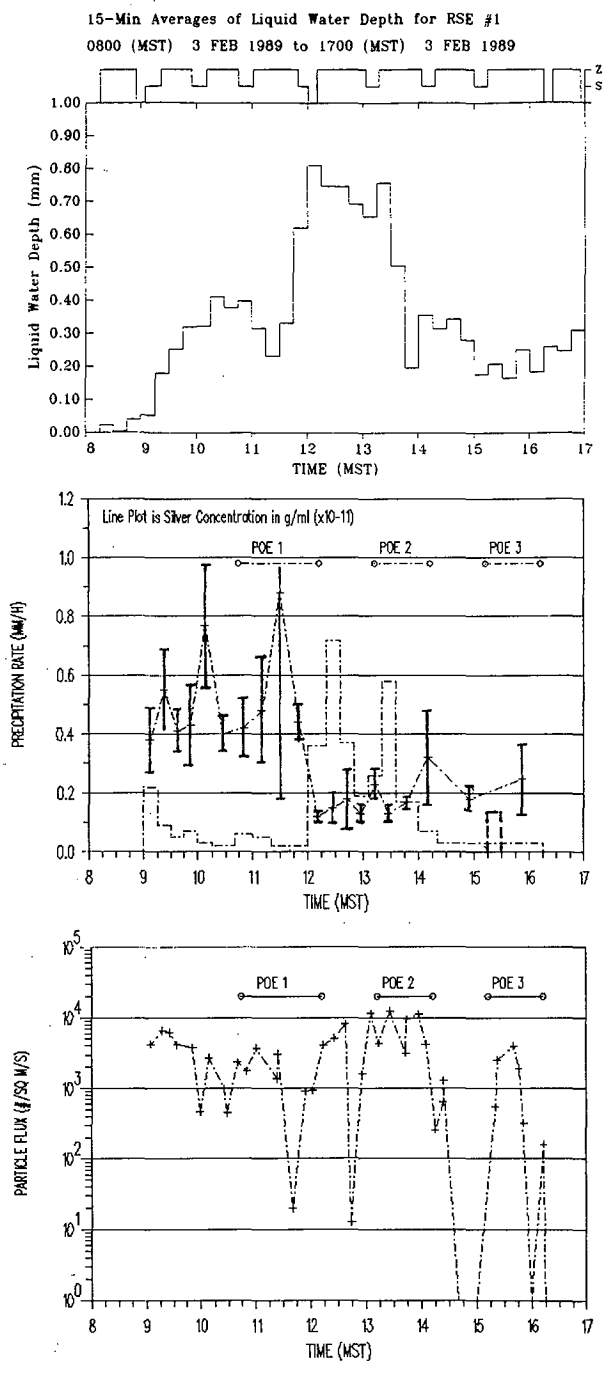

Figure 5. Time series plots of radiometer liquid water depth (top panel), precipitation rate from snow mass measurements and silver concentration in snow samples (middle panel), and ice particle flux from precipitation microphysics observations (bottom panel). Silver concentrations were obtained from the same samples used to compute precipitation rates. Step pattern on top of LW panel indicates when radiometer was in scan (s) or zenith (z) mode.

obvious seeding signatures is understandable since silver above background was not found in the snow samples collected at UGR. The season average for samples collected when no seeding occurred was 3.8×10^{-12} g ml^{-1}, with a standard deviation of 3×10^{-12} g ml^{-1}. The second panel of Fig. 5 shows that the mean Ag concentrations, with two exceptions, were uniform at 4.0 to 5.0×10^{-12} g ml^{-1} before and during POE1. The two samples with higher averages (one before and one during POE1) also had larger standard deviations, and cannot be considered significantly different. Thus for POE1, Hypothesis 2 was rejected due to the lack of a radar signature in the period prior to the arrival of the echo band. The presence of the band negated evaluation of Hypothesis 2 at the end of POE1. Also, for UGR, Hypothesis 3 was rejected due to the lack of definitive microphysical effects and the absence of silver.

3.4.2 Period of Effect 2

The reflectivity core of the mesoscale echo feature passed over UGR between the end of POE1 and the end of POE2. During this entire period a deep cloud layer existed with echo tops as high as 7 km (-32C). At 1230 the echo top began dropping, and reached 4.0 km (-12C) by 1400. The high level of background echo eliminated the possibility of detecting seeding effects in the radar data, and therefore Hypothesis 2 could not be reliably evaluated.

The 2D-C concentration increased from 10 to 100 l^{-1} on the leading edge of the precipitation band, with 40-100 l^{-1} values seen throughout the band. Within POE2 particle concentrations were nearly equal to the period (1200-1300) preceding POE2, and due to the high natural background produced by the band a seeding effect cannot be distinguished. The shift to a greater percentage of 200-600 micron particles after 1300, as total concentration declined, is not an expected seeding effect, but is consistent with the band passage.

Liquid water remained high (>0.7 mm) throughout the band passage, indicating the low level cloud was not significantly depleted of supercooled liquid at the upwind location. The drop in liquid after 1330 suggests the large values may have been due to increased convergence and vertical velocity with the band (see Sassen et al., 1990 for similar examples). At UGR the predominant ice crystal habits changed to rimed stellars, dendrites and graupel-like snow (up to 4 mm size) with the arrival of the band, but small rimed particles (<0.5 mm) were also still observed. By 1422 the larger, cold-habit particles were gone with the small rimed particles remaining (as in the shallow cloud before 1130).

As with the other data, particle number flux and precipitation rate reflected the band passage. The highest precipitation rates were 0.6-0.7 mm h^{-1} in the band core. Behind the band the rates again dropped below 0.1 mm h^{-1}. Basically, microphysical seeding effects were undetectable due to the presence of the band.

There were percentage increases in the small particle sizes and hexagonal habits throughout POE2, but as in POE1, silver concentrations were similar before and during POE2. The downward shift in average Ag concentration between 1145 and 1215 was likely due to two factors. First, the first 10 samples of RSE#1 were analyzed using one laboratory calibration based on standard samples, while the last 10 samples were based on a second calibration. Second, the level of Ag tends to be higher when the snow sample mass is very small, as was the case for the first ten samples. Based on the available data, Hypothesis 2 could not be effectively evaluated during POE2. Hypothesis 3 was rejected due to the lack of silver in the snow samples.

3.4.3 Period of Effect 3

This final period produced the most interesting sequence of events. Following POE2 a very shallow cloud (echo) existed over UGR from 1430-1545. A change in echo intensity occurred at the start of POE3 (within reasonable uncertainty in wind speed), without a significant change in echo top height. Two distinct echo maxima are obvious within POE3. Figure 4 shows that the 2D-C detected an increase in both concentration and computed precipitation rate near the beginning of POE3. Relatively large percentage increases were simultaneously noted in the 160-400 micron size categories, and in the hexagonal habit category (typical of small rimed particles). This type of 2D-C pattern was noted by Holroyd (1987) within AgI plumes. Figure 6 shows the period of POE3 in more detail; clearly showing the small-scale radar echo structure and the dominance of the hexagonal habits. This combination of events is much more consistent with the expected seeding effects.

The liquid water pattern was similar to POE1 with values at 0.2-0.3 mm. Using the 1 km cloud thickness shown by the radar, these liquid depths convert to concentrations of 0.2-0.3 g m^{-3}. Since mesoscale features were not in evidence, this liquid appears to have been generated strictly orographically. The particle flux from black velvet observations shows a very well defined peak centered in POE3, with the initial increase being coincident with the beginning of POE3. A shadowbox photograph at 1550 showed a monodispersed collection of very small (<300 microns) rimed particles. Observers at UGR noted what appeared to be a distinct plume of ice particles moving over the site from the direction of Generator Site 4. The precipitation rate at the beginning of POE3 was based on a particularly long sampling period (70 min), but the observer noted that almost all the snow in the sample fell between 1515 and 1530, which would have produced the peak shown by the dashed-line bar in Fig. 5. Except for the lack of aggregated crystals the observations matched the expected microphysical effects of seeding. The one "piece" of the seeding effects "puzzle" that does not fit is the lack of enhanced Ag concentration in the snow samples centered at 1500 and 1552. (A ten-fold increase in Ag concentration is a reasonable expectation for "seeded" snow samples.) The first sample overlapped the beginning of POE3 and could have contained natural snowfall, but as noted above the bulk of this sample came during POE3. As indicated in Section 2 the combination of implied microphysical effects without the presence of Ag above background implies that targeting failed, but effects produced by natural cloud processes occurred by chance during the POE. Our *apriori* hypotheses thus negate a seeding effect at UGR unless some mechanism other than a simple nucleation mechanism was acting.

4. SUMMARY AND CONCLUSIONS

The storm of 3-4 February 1989 provided good conditions for ground-based seeding experiments. The orographically enhanced cloud liquid exceeded 0.1 mm integrated depth throughout the seeding experiments, and in fact liquid depth averaged about 0.3 mm for a 24-hour period. Cloud bases were below the ridges containing the seeding generators, and the temperature range at generator altitudes was -6 to -10°C, within the activation range of the AgI compound used for seeding. These conditions occurred during a period of generally light precipitation and relatively warm cloud tops, although cloud tops did reach temperatures as cold as -30°C during the passage of one mesoscale feature which affected two of the three POE's.

The environment in which liquid water developed conformed to the results of prior studies in the Tushar Mtns which have shown that the best liquid events occur prefrontally with low to midlevel winds from the southwest quadrant (Rauber and Grant, 1988, and Huggins, 1989). The enhancement of liquid with the arrival of a mesoscale feature, as noted in this case, has also been documented by Sassen et al. (1990). In contrast to Sassen et al, in the present case liquid was not significantly depleted by the main precipitating portion of the mesoscale event. In general the present case also conforms to the orographic cloud model presented by Sassen et al. (1990) in that the storm remained generally inefficient in precipitation production (as noted by the persistent excess supercooled liquid water) because interaction with colder-topped seeder clouds was minimal.

In reality, data were generally insufficient to confirm Hypothesis 2, since only the radar was available to monitor in-cloud changes, and only the volume directly over the downwind target was sampled. Although radar, visual and microphysical evidence suggested a seeding signature for POE3, the lack of silver in the snow indicated the event was due to a

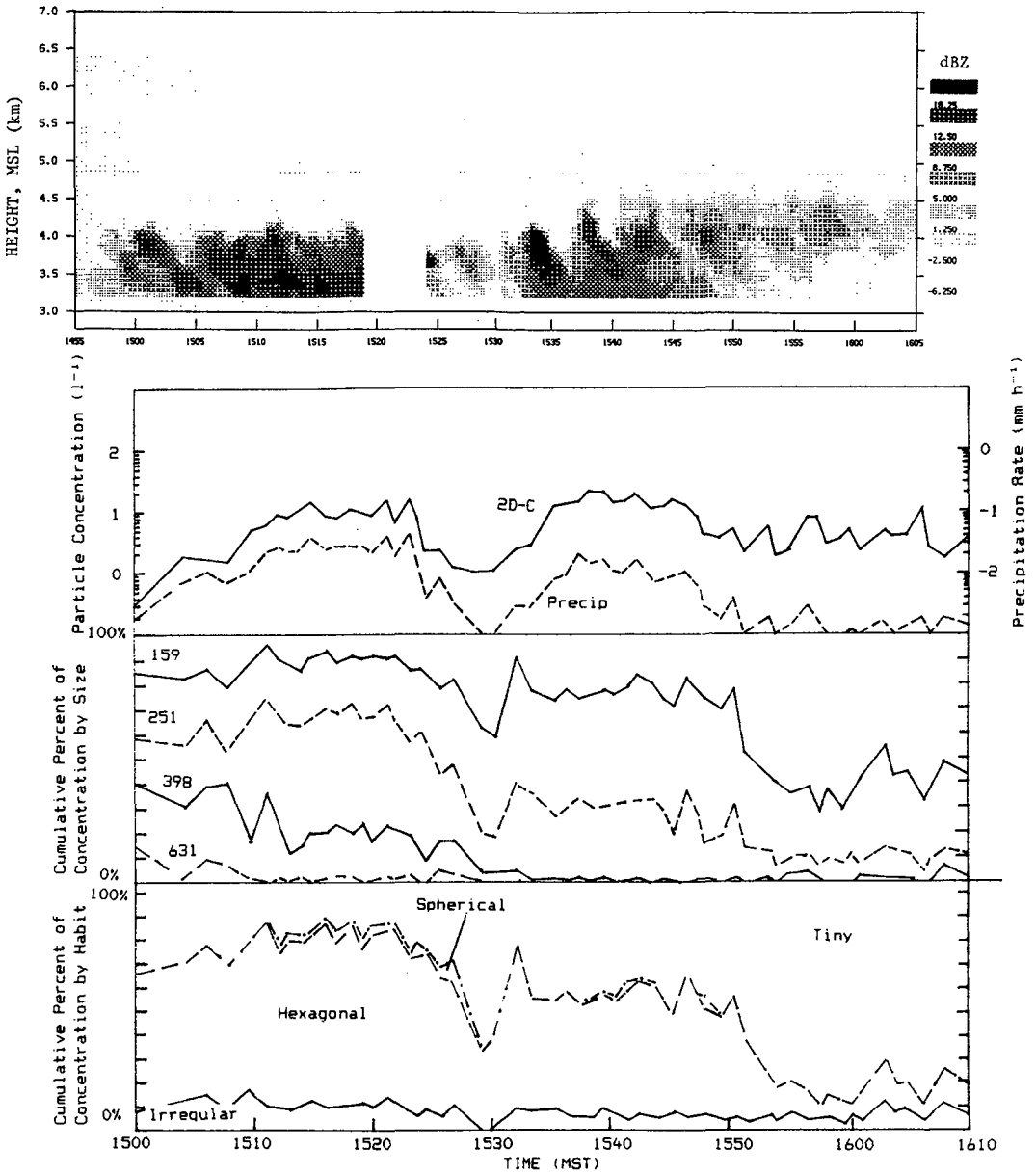

Figure 6. Same as Fig. 4, except for a time period surrounding only POE3 (1500-1600 MST).

fortuitous increase in natural ice crystal nucleation occurring in the relatively shallow and warm (-13 C cloud top) low-level orographic layer.

Some of the more probable conclusions to be drawn from the results of this experiment are: 1) Seeding effects might have occurred but UGR was not successfully targeted. Wind directions over the barrier (only marginally satisfying experimental criteria) might have been more southerly than measured by the upwind rawinsondes, thus carrying AgI-nucleated particles to the west of UGR where they sedimented out in other regions of the barrier. 2) Nucleation might have occurred instantly at the generator site (Finnegan and Pitter, 1988) allowing crystals to grow, rime in the moderately high liquid water contents observed, and fall out upwind of UGR. Other evidence of near-source effects has been reported by Heimbach and Super (1988). However, in this second scenario it is unlikely that all nuclei would have instantly activated, so that effects might also have been expected 10-20 km downwind, as noted by Super and Heimbach (1983). 3) Other options are that no silver iodide was dispensed due to remote generator malfunction, or AgI was ineffective as an ice nucleant. Based on a large number of other studies it is not likely that, if properly released, the AgI produced no ice crystals. 4) Pitter and Finnegan (1990) put forth a new idea regarding a method of secondary ice crystal production that can account for "seeding effects" without the presence of silver, when aggregation occurs in the presence of ionized salts. Although this Utah experiment offers no

direct evidence of these circumstances, the possibility might be explored in future work.

The results do point to the problems of verifying ground-based seeding experiments, and especially to the limitations of having measurements only at the source and ground target area. Given adequate funding, some improvements to the current design would include additional wind measurements in the cloudy volume between generators and target (e.g., mountaintop wind devices, scanning Doppler radar, or an acoustic Doppler device). Core sampling of snow at several locations downwind of the generators would, at a minimum, verify the release of AgI and its incorporation into the snow. Multiple tracers might separate nucleating from scavenging effects. Likewise, an ice-nucleus detector at the target could verify the release and transport of AgI with appropriate directional targeting. In fact, a sulfur hexafluoride tracer was planned for the current study, but was unavailable for the 3 February seeding experiment. One of the main problems was the lack of intermediate measurements in-cloud to verify plume location and seeding effects. The Utah/NOAA is now proceeding to experiments aimed at verification of the in-cloud processes using aircraft instrumentation, where possible, for plume tracking and microphysical studies.

5. ACKNOWLEDGEMENTS

The authors would like to thank all participants of the 1989 Utah/NOAA Field Program for their work in collecting and reducing the data sets. North American Weather Consultants provided the remote seeding generators and rawinsonde data. Special thanks to Mr. Richard Stone of DRI for providing the silver analyses. The U.S. Bureau of Reclamation provided the 2D-C probe and its data plots. The research was funded by NOAA Cooperative Agreements NA88RAH08128 and NA89RAH09090 to Utah Division of Water Resources (UDWR). Analysis efforts were funded by Contract 90-1259 between the UDWR and the Desert Research Institute, and Contract 90-1039 between UDWR and the University of Utah.

6. REFERENCES

Deshler, T., 1988: Corrections of surface particle probe measurements for the effects of aspiration. J. Atmos. Oceanic Technol., 5, 547-560.

Deshler, T., D.W. Reynolds and A.W. Huggins, 1990: Physical response of winter orographic clouds over the Sierra Nevada to airborne seeding using dry ice or silver iodide. J. Appl. Meteor., (in press).

Finnegan, W.G., and R.L. Pitter, 1988: Rapid ice nucleation by acetone-silver iodide generator aerosols. J. Wea. Mod., 20,51-53.

Fukuta, N., 1980: Development of fast falling ice crystals in clouds at -10°C and its consequence in ice phase processes. Preprints, Eighth International Conference on Cloud Physics, Clermont-Ferrand, France, 97-100.

Heimbach, J.A., Jr., and A.B. Super, 1988: The Bridger Range,Montana, 1986-1987 Snow Pack Augmentation Program. J. Wea. Mod., 20, 19-26.

Holroyd, E.W. III, 1987: Some techniques and uses of 2D-C habit classification software for snow particles. J. Atmos. Oceanic Technol., 4, 498-511.

Holroyd, E.W. III, J.T. McPartland and A.B. Super, 1988: Observations of silver iodide plumes over the Grand Mesa of Colorado. J. Appl. Meteor., 27, 1125-1144.

Huggins, A.W., 1989: Investigations of winter mountain storms in Utah during the 1987 Utah/NOAA field program. Final Report to Utah Division of Water Resources, Salt Lake City, Utah.

Long, A.B., 1984: Physical investigations of winter orographic clouds in Utah. Final Report of Utah Division of Water Resources to NOAA. Desert Research Institute, Reno, Nevada.

Long, A.B., 1986: Investigations of winter mountain storms in Utah. Final Report of Utah Division of Water Resources to NOAA. Desert Research Institute, Reno, Nevada, 350 pp.

Pitter, R.L., and W.G. Finnegan, 1990: An experimental study of effects of soluable salt impurities on ice crystal processes during growth. Atmos. Research, 25, (in press).

Prasad, N., A.R. Rodi and A.J. Heymsfield, 1989: Observations and numerical simulations of precipitation development in seeded clouds over the Sierra Nevada. J. Appl. Meteor., 28, 1031-1049.

Sassen, K., 1987: Ice cloud content from radar reflectivity. J. Climate Appl. Meteor., 26, 1050-1053.

Sassen, K., A.W. Huggins, A.B. Long, J.B. Snider and R.J. Meitin, 1990: Investigations of a winter mountain storm in Utah Part II: Mesoscale structure, supercooled liquid water development, and precipitation processes. J. Atmos. Sci., (in press).

Snider, J.B., T. Uttal and R.A. Kropfli, 1986: Remote sensor observations of winter orographic storms in southwestern Utah. NOAA Tech. Memo. ERL WPL-139, WPL, Boulder, CO. 99 pp.

Super, A.B. and B.A. Boe, 1988: Microphysical effects of wintertime cloud seeding with silver iodide over the Rocky Mountains. Part III: Observations over the Grand Mesa, Colorado. J. Appl. Meteor., 27, 1166-1182.

Super, A.B. and J.A. Heimbach, Jr.,1983: Evaluation of the Bridger Range winter cloud seeding experiment using control gages. J. Climate Appl. Metoer., 22, 1990-2011.

Super, A.B. and J.A. Heimbach, Jr., 1988: Microphysical effects of wintertime cloud seeding with silver iodide over the Rocky Mountains. Part II: Observations over the Bridger Range, Montana. J. Appl. Meteor., 27, 1152-1165.

Warburton, J.A., G.O. Linkletter, and R. Stone, 1982: The use of trace chemistry to estimate seeding effects in NHRE. J. Appl. Meteor., 21, 1089-1110.